



Hot carrier effects on Brillouin susceptibilities of semiconductor magnetoplasmas

PINKI KUMARI¹, B S SHARMA¹ and MANJEET SINGH^{2,*}

¹Department of Physics, Lords University, Chikani, Alwar 301 028, India

²Department of Physics, Government College, Matanhail 124 106, India

*Corresponding author. E-mail: manjeetgur@gmail.com

MS received 18 July 2021; revised 7 October 2021; accepted 11 October 2021

Abstract. An analytical investigation is made of hot carrier effects on real and imaginary parts of Brillouin susceptibility ($\text{Re}, \text{Im}(\chi_B)$) of semiconductor magnetoplasmas. Coupled mode approach is used to obtain expressions for $\text{Re}, \text{Im}(\chi_B)$. Numerical calculations are made for the n-InSb crystal–CO₂ laser system. Efforts are made to obtain enhanced values of $\text{Re}, \text{Im}(\chi_B)$ and change of their sign by an appropriate selection of external magnetic field (B_0) and doping concentration (n_0). The hot carrier effects of intense laser radiation modify the momentum transfer collision frequency of carriers and consequently, the nonlinearity of the medium, which in turn (i) further enhances $\text{Re}, \text{Im}(\chi_B)$, (ii) shifts the enhanced $\text{Re}, \text{Im}(\chi_B)$ towards smaller values of B_0 and (iii) widens the range of B_0 at which change of sign of $\text{Re}, \text{Im}(\chi_B)$ occurs. The change of sign of enhanced $\text{Re}, \text{Im}(\chi_B)$ of semiconductor magnetoplasmas validates the possibility of the chosen Brillouin medium as a potential candidate material for the fabrication of stimulated Brillouin scattering-dependent widely tunable and efficient optoelectronic devices such as optical switches and frequency converters.

Keywords. Brillouin susceptibility; carrier heating; magnetic field; doping; semiconductor plasmas.

PACS Nos 42.65.-k; 42.65.Es; 42.65.An; 52.38.-r; 78.55.Cr

1. Introduction

The studies of nonlinear optical susceptibilities provide important information about the nonlinearity of a medium and impart an extensive role in the fabrication of various optoelectronic devices [1–3]. In addition, the change of sign of nonlinear optical susceptibilities has interesting consequences [4,5]. The selection and operating frequency of a medium are the essential features in designing optoelectronic devices. Among the rich variety of nonlinear media, the semiconductor plasmas offer greater flexibility in the fabrication of optoelectronic devices. This is due to their compactness, provision of control of (electrons/holes) carrier relaxation time via materials designing and device structuring, operation of the devices under either oblique/normal incidence or in waveguide structures, highly advanced fabrication technology and integrating the devices with other optoelectronic components [6]. In addition, these crystals exhibit large-magnitude nonlinear optical susceptibilities in close proximity to the band-gap resonant transition regimes; which

can be further enhanced by the application of external electric/magnetic fields [7–9]. Thus, the selection of doped semiconductors as nonlinear media for the study of nonlinear optical phenomena is unquestionable.

Out of various nonlinear optical phenomena, the study of stimulated Brillouin scattering (SBS) is currently a major field of research due to its vast potentiality over a broad range of optoelectronic devices [10,11]. SBS occurs due to the scattering of laser radiation by the acoustical vibrational mode of the medium. It is a third-order optical phenomenon and its origin lies in the third-order (Brillouin) susceptibility of the medium. In the past, various aspects of Brillouin susceptibilities of semiconductor magnetoplasmas have been explored to study SBS and related phenomena by the research group of one of the present authors [12–15] and others [16]. In light of the richness of the overall performance of SBS-based optoelectronic devices, the knowledge of Brillouin susceptibility of semiconductor plasmas and its characteristic dependence on various influencing factors is essential [17].

From an extensive literature survey [10–16], it appears that no theoretical formulation has been made till now to explore the influence of hot carrier effects (HCEs) on Brillouin susceptibility in semiconductor plasmas. In the present paper, we develop a theoretical formulation followed by numerical analysis to study HCEs of intense laser radiation on real and imaginary parts of Brillouin susceptibility of semiconductor magnetoplasmas (acting as Brillouin media). The motivation for this study arises from the fact that HCEs of intense laser radiation may remarkably modify the nonlinearity of the medium and consequently the SBS process. Under high-power laser irradiation, this investigation becomes more important as it leads to a better understanding of SBS in semiconductor magnetoplasmas. Considering the origin of the phenomenon to lie in finite nonlinear induced polarisation (due to acoustical vibrational mode–laser radiation coupling) and using the coupled mode theory of interacting waves, expressions for real and imaginary parts of Brillouin susceptibility of semiconductor magnetoplasmas are obtained under hydrodynamic approximation. Efforts are made to optimise the doping level and to find appropriate values of the external magnetic field to enhance magnitudes of Brillouin susceptibilities and switching off their sign for applications in efficient optoelectronic devices, such as optical switches, frequency converters etc. Finally, a complete numerical analysis is made with a set of data available for n -InSb illuminated by a pulsed CO₂ laser.

2. Theoretical formulations

In this section, expressions are obtained for real and imaginary parts of Brillouin susceptibility (Re, Im(χ_B)) of semiconductor magnetoplasmas under hydrodynamic approximation [18] $k_a \cdot l \ll 1$, where k_a is the acoustical vibrational wavenumber and l is the mean free path of the carriers. SBS occurs due to nonlinear interaction among three coherent fields in a Brillouin medium, viz. an intense laser radiation field $E_0(x, t) = E_0 \exp[i(k_0x - \omega_0t)]$, an induced acoustical vibrational mode $u(x, t) = u_0 \exp[i(k_ax - \omega_at)]$ and scattered Stokes component of the incident laser radiation field $E_s(x, t) = E_s \exp[i(k_sx - \omega_st)]$. These fields are connected by energy and momentum phase-matching constraints $\hbar\omega_0 = \hbar\omega_a + \hbar\omega_s$ and $\hbar k_0 = \hbar k_a - \hbar k_s$, respectively. The Brillouin medium is subjected to an external magnetic field $\vec{B}_0 = \hat{z}B_0$ (i.e. perpendicular to wave vectors \vec{k}_0 , \vec{k}_a and \vec{k}_s). This configuration is known as Voigt geometry [19].

The basic equations used in the formulation of Re, Im(χ_B) are:

$$\frac{\partial^2 u(x, t)}{\partial t^2} = \frac{C}{\rho} \frac{\partial^2 u(x, t)}{\partial x^2} - 2\Gamma_a \frac{\partial u(x, t)}{\partial t} - \frac{\beta}{\rho} \frac{\partial E_1}{\partial x} + \frac{\gamma}{2\rho} \frac{\partial}{\partial x} (E_0 E_1^*) \quad (1)$$

$$\frac{\partial \vec{v}_0}{\partial t} + \nu_0 \vec{v}_0 + \left(\vec{v}_0 \cdot \frac{\partial}{\partial x} \right) \vec{v}_0 = -\frac{e}{m} [\vec{E}_0 + (\vec{v}_0 \times \vec{B}_0)] = -\frac{e}{m} (\vec{E}_e) \quad (2)$$

$$\frac{\partial \vec{v}_1}{\partial t} + \nu_0 \vec{v}_1 + \left(\vec{v}_0 \cdot \frac{\partial}{\partial x} \right) \vec{v}_1 + \left(\vec{v}_1 \cdot \frac{\partial}{\partial x} \right) \vec{v}_0 = -\frac{e}{m} [\vec{E}_1 + (\vec{v}_0 \times \vec{B}_0)] \quad (3)$$

$$\frac{\partial n_1}{\partial t} + n_0 \frac{\partial v_1}{\partial x} + n_1 \frac{\partial v_0}{\partial x} + v_0 \frac{\partial n_1}{\partial x} = 0 \quad (4)$$

$$\vec{P}_{es} = -\gamma \frac{\partial u^*}{\partial x} (\vec{E}_0) \quad (5)$$

$$\frac{\partial E_1}{\partial x} + \frac{\beta}{\varepsilon} \frac{\partial^2 u}{\partial x^2} + \frac{\gamma}{\varepsilon} \frac{\partial^2 u^*}{\partial x^2} (E_0) = -\frac{n_1 e}{\varepsilon}. \quad (6)$$

These equations have been used in analytical investigations of SBS in semiconductor-plasmas by the research group of one of the present authors [12–15]. Here, C represents the elastic stiffness constant of the Brillouin medium such that the speed of acoustical vibrational mode is given by $v_a = (C/\rho)^{1/2}$. ρ is the mass density of the Brillouin medium. To take account of acoustical damping, the term $2\Gamma_a \frac{\partial u(x, t)}{\partial t}$ is introduced in eq. (1) phenomenologically. In eq. (1), β and γ are the piezoelectric and electrostrictive coefficients of the Brillouin medium, respectively. Here, these coefficients are used phenomenologically; their effect on parametric and Brillouin nonlinearities of semiconductor-plasmas is available in [12]. E_1 represents the space-charge electric field of the Brillouin medium. n_0 (\vec{v}_0) and n_1 (\vec{v}_1) represent the carrier's equilibrium and perturbed concentrations (oscillatory fluid velocities), respectively. ν_0 stands for momentum transfer collision frequency (MTCF) of electrons. m is the effective mass of an electron. \vec{P}_{es} is the polarisation originating via the electrostrictive property of the Brillouin medium. The asterisk (*) represents the conjugate of a complex entity.

The x - and y -components of the equilibrium carrier's fluid velocity are obtained from eq. (2) as

$$v_{0x} = \frac{e(v + i\omega_0)}{m(\omega_c^2 - \omega_0^2 + 2i\nu_0\omega_0)} E_0 \quad (7a)$$

and

$$v_{0y} = \frac{\omega_c}{(v + i\omega_0)} v_{0x}. \quad (7b)$$

In eqs (7a) and (7b), $\omega_c = eB_0/m$ is the electron-cyclotron frequency.

The x - and y -components of perturbed carrier's fluid velocity can be obtained from eq. (3) by using the method adopted in ref. [20]:

$$v_{1x} = \frac{v}{(v^2 + \omega_c^2)} \left[\bar{E} - ik_0 \left(\frac{k_B T_0}{mn_0} \right) n_1 \right] \quad (8a)$$

and

$$v_{1y} = \frac{\omega_c}{(v^2 + \omega_c^2)} \left[-\bar{E} + ik_0 \left(\frac{k_B T_0}{mn_0} \right) n_1 \right]. \quad (8b)$$

In eqs (8a) and (8b),

$$\bar{E} = \frac{e}{m} (|\vec{E}_e|),$$

T_0 is the temperature of the Brillouin medium and k_B is the Boltzmann's constant.

To excite SBS, the basic need is to irradiate the Brillouin sample by an intense laser. Under the influence of the laser radiation field, the electrons (which are mobile charge carriers in n-type doped semiconductors) gain energy and their temperature reaches a value $T_e (> T_0)$. Consequently, the MTCF modifies via the relation [21]

$$v = v_0 \left(\frac{T_e}{T_0} \right)^{1/2}. \quad (9)$$

In eq. (9), the value of T_e/T_0 can be determined from energy conservation relation under steady-state operation. Following Sodha *et al* [22] and using eqs (7a) and (7b), the time-independent part of power absorbed by a single mobile charge carrier (here electron) from the laser radiation field is given by

$$\frac{e}{2} \text{Re}(\vec{v}_{0x} \cdot \vec{E}_e^*) = \frac{e^2 v_0}{2m} \frac{(\omega_c^2 - \omega_0^2)}{[(\omega_c^2 - \omega_0^2)^2 + 4v_0^2 \omega_0^2]} |\vec{E}_0|^2, \quad (10)$$

where $\text{Re}(\vec{v}_{0x} \cdot \vec{E}_e^*)$ denotes the real part of the quantity $(\vec{v}_{0x} \cdot \vec{E}_e^*)$.

Following Conwell [23], the power dissipated by a single electron from the laser radiation field in collision with polar optical phonons (POPs) is given by

$$\left(\frac{\partial \varepsilon}{\partial t} \right)_{\text{diss}} = e E_{po} (x_0)^{1/2} \kappa_0 \left(\frac{2k_B \theta_D}{m\pi} \right)^{1/2} \left(\frac{x_e}{2} \right) \cdot \exp\left(\frac{x_e}{2}\right) \cdot \frac{\exp(x_0 - x_e) - 1}{\exp(x_0) - 1}, \quad (11)$$

where

$$x_{0,e} = \frac{\hbar\omega_l}{k_B T_{0,e}},$$

in which $\hbar\omega_l$ is the energy possessed by POPs given by $\hbar\omega_l = k_B \theta_D$, where θ_D is the Debye temperature of the

Brillouin medium.

$$E_{po} = \frac{me\hbar\omega_l}{\hbar^2} \left(\frac{1}{\varepsilon_\infty} - \frac{1}{\varepsilon} \right)$$

represents the POPs' scattering potential field, in which ε and ε_∞ are the static and high-frequency dielectric constants of the Brillouin medium.

Under steady-state operation, the power absorbed by a single electron from the laser radiation field is exactly equal to the power dissipated by it in collisions with POPs. Consequently, the electron-plasma attains a steady temperature $T_e (> T_0)$. In the case of average heating of the electrons-plasma, eqs (10) and (11) yield

$$\frac{T_e}{T_0} = 1 + \alpha |\vec{E}_0|^2, \quad (12)$$

where

$$\alpha = \frac{e^2 v_0}{2m\tau\Omega_0^2} \frac{(\omega_c^2 - \omega_0^2)}{[(\omega_c^2 - \omega_0^2)^2 + 4v_0^2 \omega_0^2]},$$

in which

$$\tau = e E_{po} \kappa_0 \left(\frac{2k_B \theta_D}{m\pi} \right)^{1/2} \left(\frac{x_0}{2} \right) \frac{(x_0)^{1/2} \exp(x_0/2)}{\exp(x_0) - 1}.$$

Using eqs (9) and (11), the modified MTCF is given by

$$v = v_0 (1 + \alpha |\vec{E}_0|^2)^{1/2} \approx v_0 \left(1 + \frac{1}{2} \alpha |\vec{E}_0|^2 \right). \quad (13)$$

The laser radiation induces perturbations in electronic concentration in the Brillouin medium via piezoelectric and electrostrictive strains. The coupled equation of these perturbations, including HCEs, can be obtained by using the standard approach [24]. Differentiating eq. (4), substituting the value of E_1 from eq. (6), and for the first-order derivatives of v_0 and v_1 from eqs (2) and (3), respectively and after mathematical simplification, we obtain

$$\frac{\partial^2 n_1}{\partial t^2} + v \frac{\partial n_1}{\partial t} + \bar{\omega}_p^2 n_1 + \frac{n_0 e k_s^2 u^* (\beta \gamma \delta_1 \delta_2 A + \gamma^2 E_0^2)}{m \varepsilon_1} E_0 E_s^* = i n_1 k_s \bar{E}, \quad (14)$$

where

$$A = \frac{\omega_p^2}{(e/m)k_a},$$

$$\bar{\omega}_p = \frac{v \omega_p}{(v^2 + \omega_c^2)^{1/2}},$$

$$\delta_1 = 1 - \frac{\omega_c^2}{(\omega_0^2 - \omega_c^2)},$$

$$\delta_2 = 1 - \frac{\omega_c^2}{(\omega_s^2 - \omega_c^2)}$$

and

$$\omega_p = \left(\frac{n_0 e^2}{m \varepsilon} \right)^{1/2} \quad (\text{electron-plasma frequency}).$$

The perturbed electron concentration (n_1) may be expressed as

$$n_1 = n_{1s}(\omega_a) + n_{1f}(\omega_s),$$

where n_{1s} and n_{1f} are the low- and high-frequency components, oscillate at acoustical vibrational mode frequency ω_a and electromagnetic waves at frequencies $\omega_0 \pm p\omega_a$, in which $p = 1, 2, 3, \dots$, respectively. The electromagnetic fields at sum (i.e. $\omega_0 + p\omega_a$) and difference frequencies (i.e. $\omega_0 - p\omega_a$) are termed as anti-Stokes and Stokes modes, respectively. In the present analysis, the electron concentration perturbations at off-resonant frequencies (with $p \geq 2$) are neglected and only the first-order Stokes mode (with $p = 1$) is considered [13]. Under rotating-wave approximation (RWA), eq. (14) leads to the following coupled wave equations:

$$\begin{aligned} \frac{\partial^2 n_{1f}}{\partial t^2} + v \frac{\partial n_{1f}}{\partial t} + \bar{\omega}_p^2 n_{1f} \\ + \frac{n_0 e k_s^2 u^* (\beta \gamma \delta_1 \delta_2 A + \gamma^2 E_0^2)}{m \varepsilon} E_0 E_s^* = -i n_{1s}^* k_s \bar{E} \end{aligned} \quad (15a)$$

and

$$\frac{\partial^2 n_{1s}}{\partial t^2} + v \frac{\partial n_{1s}}{\partial t} + \bar{\omega}_p^2 n_{1s} = i n_{1f}^* k_s \bar{E}. \quad (15b)$$

Equations (15a) and (15b) show that both n_{1s} and n_{1f} are coupled to each other via laser radiation field (\bar{E}). Thus, it clearly illustrates that for SBS to take place, the presence of the laser radiation field is the pre-requisite condition.

Solving eqs (15a) and (15b) and using eq. (1), an expression for n_{1s} may be obtained as

$$\begin{aligned} n_{1s} = \frac{\varepsilon_0 n_0 k_a k_s (\beta \gamma \delta_1 \delta_2 A + \gamma^2 E_0^2)}{2 \rho \varepsilon \delta_3 (\Omega_a^2 + 2i \Gamma_a \omega_a) (\omega_0^2 - \omega_c^2 + 2i v \omega_0)} \\ \times E_0 E_s^*, \end{aligned} \quad (16)$$

where

$$\begin{aligned} \Omega_a^2 &= \omega_a^2 - k_a^2 v_a^2, \\ \delta_3 &= 1 - \frac{(\Omega_{ps}^2 - i v \omega_s)(\Omega_{pa}^2 + i v \omega_a)}{k_s^2 \bar{E}^2}, \end{aligned}$$

in which

$$\Omega_{ps}^2 = \bar{\omega}_p^2 - \omega_s^2 \quad \text{and} \quad \Omega_{pa}^2 = \bar{\omega}_p^2 - \omega_a^2.$$

The induced current density (J_{cd}) of the Brillouin medium at Stokes frequency (ω_s), including HCEs, is

obtained (by neglecting transition dipole moment) as

$$\begin{aligned} J_{cd}(\omega_s) &= n_{1s}^* e v_0 \\ &= \frac{\varepsilon_0 k_a k_s \omega_p^2 (v - i \omega_0) (\beta \gamma \delta_1 \delta_2 A + \gamma^2 E_0^2)}{2 \rho \delta_3 (\Omega_a^2 + 2i \Gamma_a \omega_a) (\omega_0^2 - \omega_c^2 + 2i v \omega_0)} \\ &\quad \times |E_0|^2 E_s^*. \end{aligned} \quad (17)$$

The nonlinear induced polarisation of the Brillouin medium (which is the time integral of the induced current density), including HCEs, is obtained as

$$\begin{aligned} P_{cd}(\omega_s) &= \int J_{cd}(\omega_s) dt \\ &= \frac{\varepsilon_0 k_a k_s \omega_p^2 \omega_0^3 (\beta \gamma \delta_1 \delta_2 A + \gamma^2 E_0^2)}{2 \rho \omega_s \delta_3 (\Omega_a^2 + 2i \Gamma_a \omega_a) (\omega_0^2 - \omega_c^2 + 2i v \omega_0)} \\ &\quad \times |E_0|^2 E_s^*. \end{aligned} \quad (18)$$

Besides $P_{cd}(\omega_s)$, the Brillouin medium also possesses a polarisation $P_{es}(\omega_s)$ originating via electrostrictive property of the Brillouin medium. Following ref. [13], and using eqs (1) and (5), we obtain

$$\begin{aligned} P_{es}(\omega_s) &= \frac{k_a k_s \omega_0^4 \gamma^2}{2 \rho (\Omega_a^2 + 2i \Gamma_a \omega_a) (\omega_0^2 - \omega_c^2 + 2i v \omega_0)} \\ &\quad \times |E_0|^2 E_s^*. \end{aligned} \quad (19)$$

Using eqs (18) and (19), the effective nonlinear induced polarisation of Brillouin medium, including HCEs, is given by

$$\begin{aligned} P(\omega_s) &= P_{cd}(\omega_s) + P_{es}(\omega_s) \\ &= \frac{k_a k_s \omega_0^3 [\varepsilon_0 \omega_p^2 (\beta \gamma \delta_1 \delta_2 A + \gamma^2 E_0^2) + \delta_3 \omega_s \omega_0 \gamma^2]}{2 \rho \delta_3 \omega_s (\Omega_a^2 + 2i \Gamma_a \omega_a) (\omega_0^2 - \omega_c^2 + 2i v \omega_0)} \\ &\quad \times |E_0|^2 E_s^*. \end{aligned} \quad (20)$$

Consequently, the effective Brillouin susceptibility of the Brillouin medium, including HCEs, is given by

$$\begin{aligned} \chi_B &= \frac{k_a k_s \omega_0^3 [\varepsilon_0 \omega_p^2 (\beta \gamma \delta_1 \delta_2 A + \gamma^2 E_0^2) + \delta_3 \omega_s \omega_0 \gamma^2]}{2 \rho \varepsilon_0 \delta_3 \omega_s (\Omega_a^2 + 2i \Gamma_a \omega_a) (\omega_0^2 - \omega_c^2 + 2i v \omega_0)}. \end{aligned} \quad (21)$$

Equation (21) reveals that χ_B is a complex quantity and it can be put forward as

$$\chi_B = \text{Re}(\chi_B) + i \text{Im}(\chi_B),$$

where $\text{Re}(\chi_B)$ and $\text{Im}(\chi_B)$ stand for real and imaginary parts of the complex χ_B . Rationalising eq. (21), we obtain

$$\text{Re}(\chi_B) = \frac{k_a k_s \omega_0^3 [\Omega_a^2 (\omega_0^2 - \omega_c^2) - 4v \Gamma_a \omega_a \omega_0] [\varepsilon_0 \omega_p^2 (\beta \gamma \delta_1 \delta_2 A + \gamma^2 E_0^2) + \delta_3 \omega_s \omega_0 \gamma^2]}{2\rho \varepsilon_0 \delta_3 \omega_s (\Omega_a^4 + 4\Gamma_a^2 \omega_a^2) [(\omega_0^2 - \omega_c^2)^2 + 4v^2 \omega_0^2]} \quad (22a)$$

$$\text{Im}(\chi_B) = \frac{k_a k_s \omega_0^3 [v \omega_0 \Omega_a^2 + \Gamma_a \omega_a (\omega_0^2 - \omega_c^2)] [\varepsilon_0 \omega_p^2 (\beta \gamma \delta_1 \delta_2 A + \gamma^2 E_0^2) + \delta_3 \omega_s \omega_0 \gamma^2]}{\rho \varepsilon_0 \delta_3 \omega_s (\Omega_a^4 + 4\Gamma_a^2 \omega_a^2) [(\omega_0^2 - \omega_c^2)^2 + 4v^2 \omega_0^2]} \quad (22b)$$

Equations (22a) and (22b) show that both $\text{Re}(\chi_B)$ as well as $\text{Im}(\chi_B)$ are influenced by the parameters β , γ , n_0 (via ω_p) and B_0 (via ω_c). $\text{Im}(\chi_B)$ accounts for a nonlinear absorption coefficient while $\text{Re}(\chi_B)$ accounts for a nonlinear index of refraction of the chosen Brillouin medium. The knowledge of nonlinear absorption coefficient and index of refraction of the Brillouin medium provide information about the design of various optoelectronic devices including amplifiers, oscillators, filters and couplers [25].

3. Results and discussion

For numerical analysis, we choose an n-type doped InSb crystal at 77 K as a Brillouin medium and illuminated it by a pulsed CO₂ laser at 10.6 μm wavelength. At 77 K, the absorption coefficient of the chosen Brillouin medium is negligible (around 10 μm wavelength) and the effects of band-to-band transitions can be ignored safely [26]. The material parameters of the n-InSb–CO₂ laser system are as follows [13]: $m = 0.014m_0$; m_0 is the electron's rest mass, $\rho = 5.8 \times 10^3 \text{ kg m}^{-3}$, $\varepsilon = 17.8$, $\varepsilon_\infty = 15.68$, $v_a = 4 \times 10^3 \text{ m s}^{-1}$, $\beta = 0.054 \text{ Cm}^{-2}$, $\gamma = 5 \times 10^{10} \text{ s}^{-1}$, $\Gamma_a = 2 \times 10^{10} \text{ s}^{-1}$, $v_0 = 3.5 \times 10^{11} \text{ s}^{-1}$, $\omega_a = 2 \times 10^{11} \text{ s}^{-1}$, $\omega_0 = 1.78 \times 10^{14} \text{ s}^{-1}$, $T_0 = 77 \text{ K}$, $\theta_D = 278 \text{ K}$.

Equations (22a) and (22b) represent Re , $\text{Im}(\chi_B)$ of the Brillouin medium by including HCEs. The expressions for Re , $\text{Im}(\chi_B)$ of the Brillouin medium by excluding HCEs can be obtained by simply replacing v by v_0 (at $T_e = T_0$) in these equations. The dependence of Re , $\text{Im}(\chi_B)$ on external magnetic field B_0 (via ω_c) and doping concentration n_0 (via ω_p) by excluding and including HCEs are explored. The aim is to: (i) determine appropriate values of B_0 and n_0 to enhance Re , $\text{Im}(\chi_B)$ and (ii) search for the usefulness of efficient optoelectronic devices based on Brillouin nonlinearities.

In figures 1a and 1b, Re , $\text{Im}(\chi_B)$ vs. magnetic field B_0 are plotted for the cases: (i) without HCEs and (ii) with HCEs. These clearly show the substantial enhancements of Re , $\text{Im}(\chi_B)$ as well as change of their sign. The situation at which Re , $\text{Im}(\chi_B)$ alter their sign is termed as ‘cut-off’ or ‘dielectric anomaly’ [27].

When HCEs are excluded, with increasing B_0 , $\text{Re}(\chi_B)$ is positive while $\text{Im}(\chi_B)$ is negative, vanishingly small,

and remain independent of magnetic field for $0 \leq B_0 \leq 2.5 \text{ T}$. The nature of the curves of both Re , $\text{Im}(\chi_B)$ are very sensitive in the regime $2.5 \text{ T} < B_0 < 4.5 \text{ T}$. In this regime, with rising B_0 , $\text{Re}(\chi_B)$ starts increasing while $\text{Im}(\chi_B)$ starts decreasing, achieving a peak positive value ($\text{Re}(\chi_B) = 3 \times 10^{-17} \text{ m}^2 \text{ V}^{-2}$) and a peak negative value ($\text{Im}(\chi_B) = -6 \times 10^{-17} \text{ m}^2 \text{ V}^{-2}$), respectively at $B_0 = 3.4 \text{ T}$. By slightly increasing B_0 beyond this value, $\text{Re}(\chi_B)$ starts sharply decreasing while $\text{Im}(\chi_B)$ starts sharply increasing. At $B_0 = 3.5 \text{ T}$, both Re , $\text{Im}(\chi_B)$ vanish. With further increase in B_0 beyond this value, both Re , $\text{Im}(\chi_B)$ alter their sign achieving a peak negative value ($\text{Re}(\chi_B) = -6 \times 10^{-16} \text{ m}^2 \text{ V}^{-2}$) and peak positive value ($\text{Im}(\chi_B) = 2 \times 10^{-15} \text{ m}^2 \text{ V}^{-2}$), respectively at $B_0 = 3.6 \text{ T}$. For $3.6 \text{ T} < B_0 < 4.5 \text{ T}$, $\text{Re}(\chi_B)$ increases sharply while $\text{Im}(\chi_B)$ decreases sharply. For $4.5 \text{ T} \leq B_0 \leq 10 \text{ T}$, $\text{Re}(\chi_B)$ remains negative while $\text{Im}(\chi_B)$ remains positive and vanishingly small. The nature of the curves of both Re , $\text{Im}(\chi_B)$ is again repeated in the regime $10.8 \text{ T} < B_0 < 11.8 \text{ T}$ like the regime $2.5 \text{ T} < B_0 < 4.5 \text{ T}$. The regime $11.8 \text{ T} \leq B_0 \leq 13.2 \text{ T}$, $\text{Re}(\chi_B)$ remains negative while $\text{Im}(\chi_B)$ remains positive and vanishingly small. This distinct behaviour of Re , $\text{Im}(\chi_B)$ occurs due to the following resonance conditions: (i) $(\omega_p^2 \omega_c^2)/v^2 \sim \omega_s^2$ and (ii) $v^2 \omega_p^2/(v^2 + \omega_c^2) \sim \omega_s^2$. An important aspect of these resonance conditions is the interaction between electron–plasmon mode and electron–cyclotron mode. Let us define this as coupled plasmon–cyclotron mode. When the laser radiation field interacts with this coupled mode, the coupled mode frequency-dependent Stokes mode is generated. Here, it is beneficial to shift the scattered Stokes mode frequency to an achievable spectral regime in proportion to ω_p (or n_0) for fixed ω_c (or B_0), ω_c (or B_0) for fixed ω_p (or n_0), and a combination of both ω_c and ω_p . Continuously increasing n_0 (via ω_p) and decreasing B_0 (via ω_c) in the same proportion maintains the resonance conditions at a fixed value of ω_s . Further, by continuously increasing n_0 and decreasing B_0 without maintaining their proportion, shifts the value of ω_s . At $B_0 = 14.2 \text{ T}$, a change of sign of both Re , $\text{Im}(\chi_B)$ is observed due to resonance condition and (iii) $\omega_c^2 \sim \omega_0^2$. This resonance condition is independent of ω_p (or n_0).

When HCEs are included, the features of $\text{Re}(\chi_B)$ – B_0 and $\text{Im}(\chi_B)$ – B_0 plots remain unchanged except that:

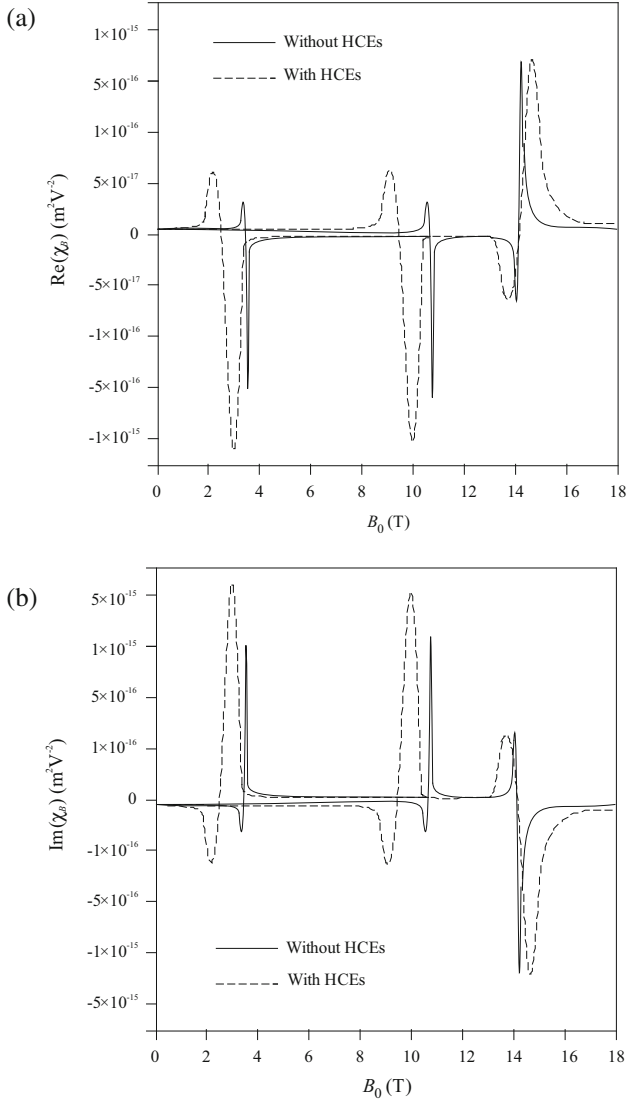


Figure 1. (a) Plot of $\text{Re}(\chi_B)$ vs. B_0 for cases: (i) without HCEs and (ii) with HCEs for $n_0 = 2 \times 10^{19} \text{ m}^{-3}$ and $E_0 = 7 \times 10^7 \text{ V m}^{-1}$ and (b) plot of $\text{Im}(\chi_B)$ vs. B_0 for cases (i), (ii) and for parameters given in figure 1a.

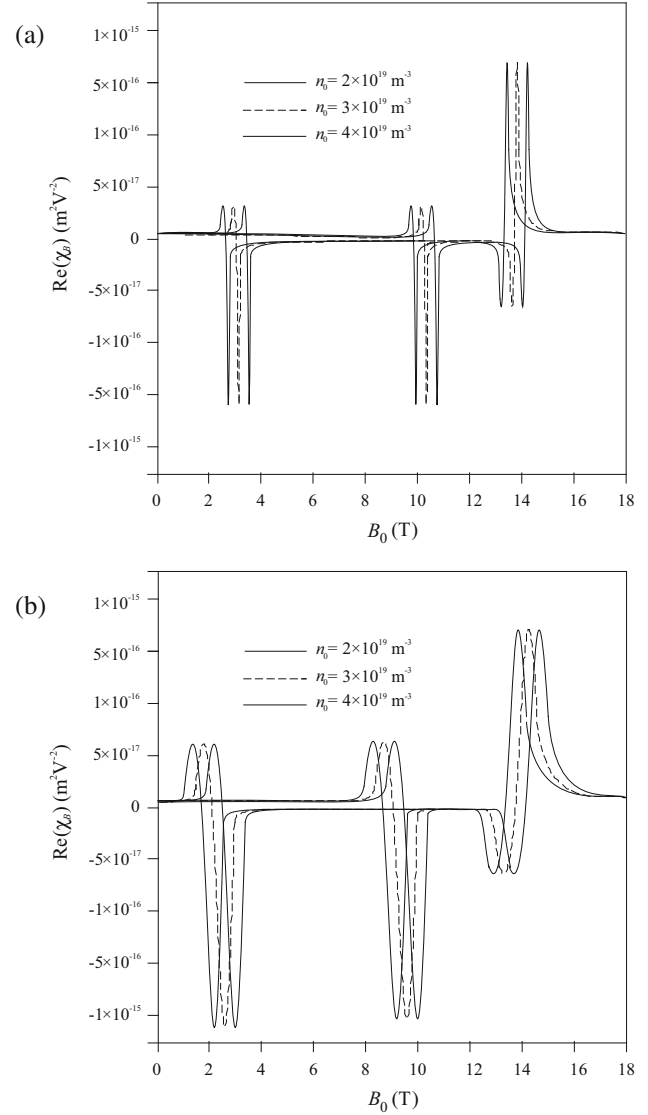


Figure 2. (a) Plot of $\text{Re}(\chi_B)$ vs. B_0 by excluding HCEs for three different doping concentrations ($n_0 = 2 \times 10^{19} \text{ m}^{-3}$, $3 \times 10^{19} \text{ m}^{-3}$ and $4 \times 10^{19} \text{ m}^{-3}$) at $E_0 = 7 \times 10^7 \text{ Vm}^{-1}$ and (b) plot of $\text{Re}(\chi_B)$ vs. B_0 by including HCEs for the parameters given in figure 2a.

1. the change of sign of Re , $\text{Im}(\chi_B)$ previously occurred at $B_0 = 3.5 \text{ T}$ and 10.8 T have now been shifted to $B_0 = 2.5 \text{ T}$ and 9.8 T , respectively;
2. the peak positive and negative values of Re , $\text{Im}(\chi_B)$ occurring due to resonance conditions (i) and (ii) have been enhanced almost five times;
3. the range at which the change of sign occurs has been widened.
4. The magnitude of Re , $\text{Im}(\chi_B)$ remains unaltered at resonance condition (iii) by including HCEs; rather this resonance condition shifts the value of B_0 at which resonance occurs towards lower values and widens the range of B_0 at which change of sign of both Re , $\text{Im}(\chi_B)$ occur.

Around resonances, the electron's drift velocity (which is a function of B_0) increases, attains a value higher than acoustical vibrational mode and due to this the rate of energy flow from the laser radiation field to acoustical vibrational mode increases, and consequently the amplification of acoustical vibrational mode takes place in the Brillouin medium. Eventually, the interaction between the laser radiation field and amplified acoustical vibrational mode enhances the amplitude of scattered Stokes mode.

The most significant feature of the result is the monitoring of Re , $\text{Im}(\chi_B)$ by properly selecting B_0 and also attaining large values in a Brillouin medium consisting

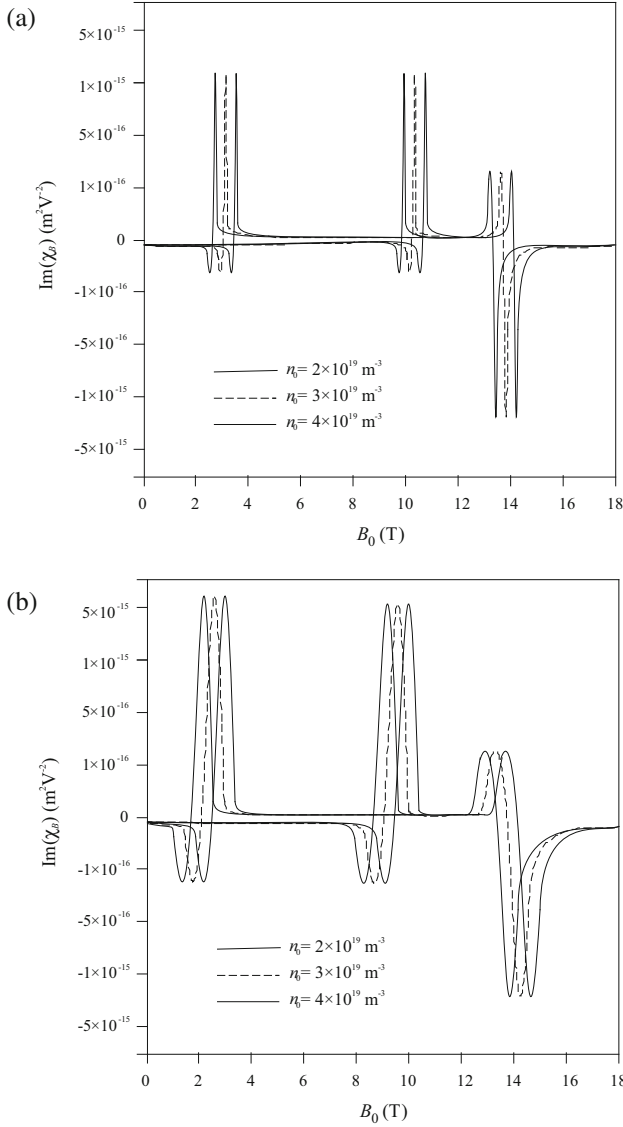


Figure 3. (a) Plot of $\text{Im}(\chi_B)$ vs. B_0 by excluding HCEs for the parameters given in figure 2a and (b) plot of $\text{Im}(\chi_B)$ vs. B_0 by including HCEs for the parameters given in figure 2a.

of semiconductor magnetoplasmas. The results obtained in figures 1a and 1b permit the tuning of scattered Stokes mode over a broad frequency regime and reveal a strong possibility of fabrication of frequency converters.

In figures 2a and 2b, $\text{Re}(\chi_B)$ vs. magnetic field B_0 is plotted by excluding and including HCEs, respectively for three different doping concentrations ($n_0 = 2 \times 10^{19} \text{ m}^{-3}$, $3 \times 10^{19} \text{ m}^{-3}$ and $4 \times 10^{19} \text{ m}^{-3}$) at $E_0 = 7 \times 10^7 \text{ V m}^{-1}$. These give a picture of the enhancement of $\text{Re}(\chi_B)$ as well as change of its signs. For a fixed n_0 , the nature of curves is similar to the ones obtained in figure 1a. An increase in n_0 does not alter the magnitude of peak positive and negative values of $\text{Re}(\chi_B)$, rather it shifts the value of B_0 at which

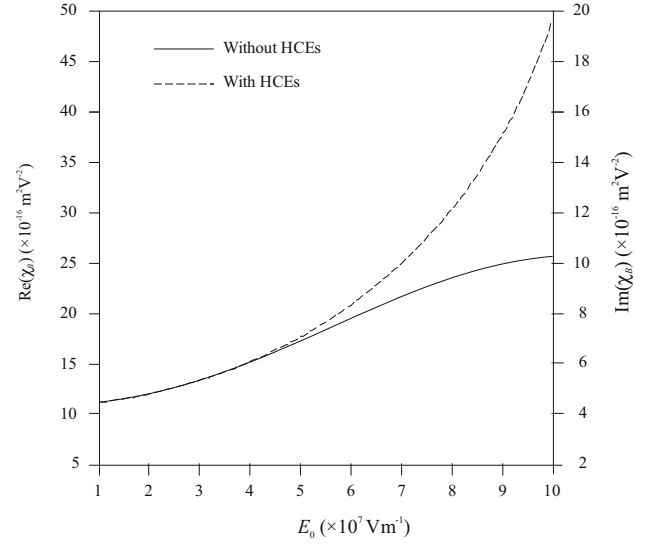


Figure 4. Plot of $\text{Re}(\chi_B)$, $\text{Im}(\chi_B)$ vs. E_0 at $B_0 \approx 14.2 \text{ T}$ for the cases (i) and (ii) given in figure 1a.

change of sign of $\text{Re}(\chi_B)$ occurs towards lower values. A comparison between results of figures 2a and 2b reveals that for a fixed n_0 , the HCEs induced by laser radiation widen the range of B_0 at which the change of sign of $\text{Re}(\chi_B)$ occurs; a result which supports the results of figure 1a.

In figures 3a and 3b, $\text{Im}(\chi_B)$ vs. magnetic field B_0 is plotted by excluding and including HCEs, respectively for the parameters given in figures 2a and 2b. These give a picture of the enhancement of $\text{Im}(\chi_B)$ as well as change of its signs. For a fixed n_0 , the nature of curves is similar to that obtained in figure 1b. An increase in n_0 does not alter the magnitude of peak positive and negative values of $\text{Im}(\chi_B)$, rather it shifts the value of B_0 at which change of sign of $\text{Im}(\chi_B)$ occurs towards lower values. A comparison between the results of figures 3a and 3b reveals that for a fixed n_0 , the HCEs induced by intense laser radiation widens the range of B_0 at which the change of sign of $\text{Im}(\chi_B)$ occurs; a result which supports the results of figure 1b.

From eqs (22a) and (22b), it can be seen that apart from magnetic field dependence, laser radiation field strength can also be employed to enhance $\text{Re}(\chi_B)$, $\text{Im}(\chi_B)$. In figure 4, both $\text{Re}(\chi_B)$, $\text{Im}(\chi_B)$ vs. laser radiation field amplitude E_0 are plotted for cases (i) without HCEs and (ii) with HCEs. It can be seen that both $\text{Re}(\chi_B)$, $\text{Im}(\chi_B)$ exhibit similar nature of curves throughout the plotted range of E_0 such that $\text{Re}(\chi_B) = 2.5\text{Im}(\chi_B)$. When HCEs are included, the shape of the curve is a parabola. For smaller values of E_0 ($< 4 \times 10^7 \text{ V m}^{-1}$) when HCEs are insignificant, both $\text{Re}(\chi_B)$, $\text{Im}(\chi_B)$ increase in a parabolic shape with increasing E_0 . However, they

gradually start deviating from the parabolic shape as HCEs become significant, in the region $E_0 \geq 4 \times 10^7$ V m⁻¹. Both Re, Im(χ_B) become almost independent of E_0 beyond $E_0 \approx 10^8$ V m⁻¹ and it is evident from this figure that both Re, Im(χ_B) become almost double when HCEs are included in comparison to when they are excluded. This behaviour can be easily understood in terms of the temperature dependence of Re, Im(χ_B) via MTCF in eqs (22a) and (22b). This deviation of the behaviour of the Brillouin susceptibilities, from their usual parabolic shape, at high laser radiation fields, emphasises the necessity for inclusion of HCEs in SBS processes.

4. Conclusions

In the present paper, a theoretical formulation followed by numerical analysis is made to study HCEs on real and imaginary parts of Brillouin susceptibility of semiconductor magnetoplasmas. The analysis enables one to draw the following conclusions:

1. The semiconductor fluid model is used very fruitfully to study the influence of HCEs of intense laser radiation on Re, Im(χ_B) of semiconductor magnetoplasmas.
2. The analysis offers three achievable resonance conditions: (i) $(\omega_p^2 \omega_c^2)/v^2 \sim \omega_s^2$, (ii) $v^2 \omega_p^2/(v^2 + \omega_c^2) \sim \omega_s^2$ and (iii) $\omega_c^2 \sim \omega_0^2$, at which significant enhancement as well as change of sign of Re, Im(χ_B) occurs. Resonance conditions (i) and (ii) offer the tuning of scattered Stokes Brillouin mode over a wide range of frequencies by properly controlling the doping level and/or external magnetic field.
3. The HCEs of intense laser radiation (a) enhance the peak positive and negative values of Re, Im(χ_B) considerably, (b) shift the enhanced peak positive and negative values of Re, Im(χ_B) towards lower values of magnetic field and (c) widen the range of magnetic field at which the change of sign of Re, Im(χ_B) occurs.
4. For laser radiation field amplitude $E_0 < 4 \times 10^7$ V m⁻¹, HCEs on Re, Im(χ_B) are absent. However, for $E_0 \geq 4 \times 10^7$ V m⁻¹, HCEs become significant and more pronounced at higher values of E_0 .
5. The technological potentiality of semiconductor magnetoplasmas as the hosts for the fabrication of SBS-dependent widely tunable and efficient optoelectronic devices such as optical switches and frequency converters.

Acknowledgements

The authors are very thankful to the learned referee for many useful suggestions in the English language corrections for improving the quality of this paper. They are also thankful to Prof. Sudhir Kumar, Department of English and Foreign Languages, M.D. University, Rohtak, India for careful reading of the revised manuscript.

References

- [1] H J Gerritsen, *Appl. Phys. Lett.* **10**, 239 (1967)
- [2] B I Stepanov, E V Ivakin and A G Rubanov, *Dok. Acad. Nauk. SSSR* **196**, 567 (1971)
- [3] A Yariv and P Yeh, *Optical waves in crystals* (Wiley, New York, 1984)
- [4] G Banfi, V Degiorgio and D Ricard, *Adv. Phys.* **47**, 447 (1998)
- [5] H Haug and S W Koch, *Quantum theory of the optical and electronic properties of semiconductors*, 4th edn (World Scientific, Singapore, 2004)
- [6] S Mokkaapati and C Jagadish, *Mater. Today* **12**, 22 (2009)
- [7] D A B Miller, *Laser Focus* **19**, 61 (1983)
- [8] Sandeep, S Dahiya and N Singh, *Mod. Phys. Lett. B* **31**, 1750294 (2017)
- [9] S Bhan, H P Singh, V Kumar and M Singh, *Optik – Int. J. Light Electron Opt.* **184**, 467 (2019)
- [10] E Garmire, *New J. Phys.* **19**, 011003 (2017)
- [11] Z Bai, H Yuan, Z Liu, P Xu, Q Gao, R J Williams, O Kitzler, R P Mildren, Y Wang and Z Lu, *Opt. Mater.* **75**, 626 (2018)
- [12] M Singh, P Aghamkar, N Kishore and P K Sen, *J. Nonlin. Opt. Phys. Mater.* **15**, 465 (2006)
- [13] P Aghamkar, M Singh, N Kishore, S Duhan and P K Sen, *Semicond. Sci. Technol.* **22**, 749 (2007)
- [14] M Singh and P Aghamkar, *Opt. Commun.* **281**, 1251 (2008)
- [15] M Singh, P Aghamkar, N Kishore and P K Sen, *Opt. Laser Technol.* **40**, 215 (2008)
- [16] C Uzma, I Zeba, H A Shah and M Salimullah, *J. Appl. Phys.* **105**, 013307 (2009)
- [17] E Garmire, *Int. J. Opt.* **2018**, 2459501 (2018)
- [18] S G Chefranov and A S Chefranov, Hydrodynamic methods and exact solutions in applications to the electromagnetic field theory in medium, in: *Nonlinear optics – Novel results in field theory in medium* edited B Lemberikov (Intechopen, UK, 2020)
- [19] G C Aers and A D Boardman, *J. Phys. C: Solid State Phys.* **11**, 945 (1978)
- [20] G Sharma and S Ghosh, *Phys. Status Solidi A* **184**, 443 (2001)
- [21] A C Beer, *Galvanometric effects in semiconductors: Solid state physics* (Academic Press, New York, 1963) Suppl. 9

- [22] M S Sodha, A K Ghatak and V K Tripathi, *Self-focusing of laser beams in dielectrics, plasmas and semiconductors* (Tata McGraw-Hill, New Delhi, 1974) pp. 55–62
- [23] E M Conwell, *High field transport in semiconductors* (Academic Press, New York, 1967) p. 159
- [24] N Nimje, S Dubey and S Ghosh, *Chin. J. Phys.* **49**, 901 (2011)
- [25] V E Gusev and A A Karabutov, *Laser optoacoustics* (American Institute of Physics, New York, 1993)
- [26] P Y Yu and M Cardona, Vibrational properties of semiconductors, and electron-phonon interactions, in: *Fundamentals of semiconductors, Graduate texts in physics* (Springer, Berlin, Heidelberg, 2010)
- [27] E D Palik and J K Furdyna, *Rep. Prog. Phys.* **33**, 1193 (1970)